

# SCIENTIFIC REPORTS



OPEN

## Future global productivity will be affected by plant trait response to climate

Nima Madani<sup>1,2</sup>, John S. Kimball<sup>1,2</sup>, Ashley P. Ballantyne<sup>2</sup>, David L. R. Affleck<sup>3</sup>, Peter M. van Bodegom<sup>4</sup>, Peter B. Reich<sup>5,6</sup>, Jens Kattge<sup>7,8</sup>, Anna Sala<sup>9</sup>, Mona Nazeri<sup>10</sup>, Matthew O. Jones<sup>1</sup>, Maosheng Zhao<sup>11</sup> & Steven W. Running<sup>1,2</sup>

Plant traits are both responsive to local climate and strong predictors of primary productivity. We hypothesized that future climate change might promote a shift in global plant traits resulting in changes in Gross Primary Productivity (GPP). We characterized the relationship between key plant traits, namely Specific Leaf Area (SLA), height, and seed mass, and local climate and primary productivity. We found that by 2070, tropical and arid ecosystems will be more suitable for plants with relatively lower canopy height, SLA and seed mass, while far northern latitudes will favor woody and taller plants than at present. Using a network of tower eddy covariance CO<sub>2</sub> flux measurements and the extrapolated plant trait maps, we estimated the global distribution of annual GPP under current and projected future plant community distribution. We predict that annual GPP in northern biomes ( $\geq 45^\circ\text{N}$ ) will increase by 31% ( $+8.1 \pm 0.5 \text{ Pg C}$ ), but this will be offset by a 17.9% GPP decline in the tropics ( $-11.8 \pm 0.84 \text{ Pg C}$ ). These findings suggest that regional climate changes will affect plant trait distributions, which may in turn affect global productivity patterns.

Climate change is expected to significantly influence global species distributions in the next decades<sup>1,2</sup>, which raises the question of how these changes may affect dominant plant community traits and ecosystem productivity. The response of species to climate change can vary from extinction to resilience<sup>3</sup>. However, plant species may also adapt to climate change by altering their physical traits<sup>3</sup> or by relocating to regions with more suitable environmental conditions<sup>4,5</sup>. Increases in shrub dominance in the tundra<sup>6</sup> and declines in taller, larger diameter trees in California in the last century, inducing a shift toward oak dominance over historic pine dominance<sup>7</sup>, provide recent examples of such changes.

Temperature, water supply and solar radiation are primary climatic factors constraining ecosystem productivity at global scales<sup>8,9</sup> such that each or a combination of these factors limits vegetation growth within global biomes defined by species with distinctive traits and/or life history strategies. From the ecosystem process perspective, vegetation productivity has increased in recent decades<sup>8,10</sup>. Plant productivity may be enhanced through direct fertilization effects from increasing atmospheric CO<sub>2</sub> concentrations<sup>11,12</sup>. However, concomitant changes in temperature and rainfall can also alter productivity by extending the growing season in cold regions, while limiting productivity in warmer and drier regions<sup>13</sup>. A key, unresolved question is how changes in precipitation and temperature will affect species functional traits and what impact changes in traits and plant communities will have on patterns of global productivity.

<sup>1</sup>Numerical Terradynamic Simulation Group, W.A. Franke College of Forestry & Conservation, University of Montana, Missoula, MT, 59812 USA. <sup>2</sup>Department of Ecosystem and Conservation Sciences, W.A. Franke College of Forestry & Conservation, University of Montana, Missoula, Montana, 59812 USA. <sup>3</sup>Department of Forest Management, W.A. Franke College of Forestry & Conservation, University of Montana, 32 Campus Drive, Missoula, MT, 59812, USA. <sup>4</sup>Institute of Environmental Sciences (CML), University Leiden, 2333CC, Leiden, The Netherlands. <sup>5</sup>Department of Forest Resources, University of Minnesota, 1530 Cleveland Avenue North, St. Paul, Minnesota, 55108, USA. <sup>6</sup>Hawkesbury Institute for the Environment, Western Sydney University, Penrith, 2753 NSW, Australia. <sup>7</sup>Max-Planck-Institute for Biogeochemistry, 07745, Jena, Germany. <sup>8</sup>German Centre for Integrative Biodiversity Research (iDiv) Halle-Jena-Leipzig, 04103, Leipzig, Germany. <sup>9</sup>Division of Biological Sciences, University of Montana, Missoula, MT, 59812, USA. <sup>10</sup>Department of Wildlife, Fisheries and Aquaculture, Mississippi State University, MS, 39762, USA. <sup>11</sup>Department of Geographical Sciences, University of Maryland, College Park, Maryland, 20742, USA. Correspondence and requests for materials should be addressed to N.M. (email: [nima.madani@ntsg.umt.edu](mailto:nima.madani@ntsg.umt.edu))

Plant traits have been shown to provide important information about ecosystem structure and productivity<sup>14</sup>. Plants have distinctive strategies that manifest as functional traits adapted to local habitats and environmental conditions<sup>15,16</sup>, and yet trade-offs among functional traits can reveal and influence ecosystem processes<sup>14,17–19</sup>. Leaf traits such as leaf nitrogen content (N) and SLA (the ratio of leaf area per unit dry mass,  $\text{m}^2 \text{kg}^{-1}$ ) influence canopy photosynthetic capacity<sup>20</sup> and have been shown to improve understanding of key ecosystem processes such as GPP<sup>21,22</sup>. SLA, vegetation height, and seed mass are among the most widely used plant traits in ecological studies and can explain species distributions<sup>16,23,24</sup>. The leaf-height-seed (LHS) relationship was proposed to help explain species co-existence strategies: while height and seed mass reflect capabilities to cope with environmental disturbance, SLA distinguishes between competitors and stress-tolerators<sup>16</sup>. The LHS relationship is also related to ecosystem function. Leaves with higher SLA generally have higher nutrient (N) concentrations<sup>15,17,19</sup>, leading to higher carbon assimilation<sup>22</sup> and respiration<sup>25</sup>. Species with higher seed mass are generally found in more productive regions<sup>26–28</sup> and can tolerate a higher degree of stresses, while species with lower seed mass need relatively less energy for seed production<sup>29</sup>. Taller trees tend to have greater access to light, deploy more canopy leaf area and have higher leaf nitrogen content<sup>30,31</sup>.

Despite the influence of morphological plant traits on ecosystem properties and function, their role in global ecosystem process models is often neglected or not properly captured<sup>21</sup>. Many global models use generalized plant functional type (PFT) categories to explain differences in ecosystem function<sup>22</sup>. While these functional types are distinguishable using physical plant traits<sup>23</sup>, large variability in ecosystem function within individual PFT classes<sup>22,32</sup> suggests that such broad categories are insufficient in modeling ecosystem processes such as productivity. Such uncertainty may contribute to the large range of estimated global annual GPP (106–175  $\text{Pg C yr}^{-1}$ ) from different models<sup>33–36</sup>. However, recent attempts to map global plant traits<sup>23</sup>, the effect of future climate conditions on community trait patterns<sup>37</sup>, and incorporation of plant trait information into earth system models<sup>38,39</sup> have improved our understanding of climate impacts on plant community patterns and ecosystem productivity.

In this research we characterize the relationships between bioclimatic variables and plant traits using a global plant trait database (TRY)<sup>40</sup>. Specifically, we analyze relationships between gridded bioclimatic factors related to precipitation and temperature, and selected key dominant community plant traits. Via analyses of annual GPP derived from 164 globally distributed carbon flux towers, we show that ecosystem productivity is significantly related to the plant trait observations. We then use selected bioclimatic variables<sup>41</sup> from 17 global Earth System Models (ESMs) of the Intergovernmental Panel on Climate Change (IPCC) Coupled Model Intercomparison Project Phase 5 (CMIP5) based on the Representative Concentration Pathway (RCP) 8.5<sup>42</sup> for the year 2070 to predict changes in key plant traits under projected future climate change. We find that changes in ecosystem suitability favor plants with certain functional traits, and that projected climate change will impact both productivity and underlying community dominant functional traits.

## Results and Discussion

We used a Generalized Additive Model (GAM)<sup>43</sup> to explain variability in species trait observations (Figure S2) relative to selected bioclimatic variables. The bioclimatic variables selected are based on stepwise variable selection and the best performance [Akaike's Information Criterion (AIC)<sup>44</sup> and lowest Root Mean Squared Errors (RMSE)] indicated from a leave-one-out cross validation analysis. Among the 19 available climatic variables analyzed from the WorldClim database<sup>41</sup>, SLA is mainly explained by annual average precipitation, maximum temperature of the warmest month and minimum temperature of the coldest month. Based on covariate analysis of the global GAM, SLA is proportional to precipitation (P) except for moist climates ( $P > \sim 1000 \text{ mm yr}^{-1}$ ) where SLA is relatively insensitive to further P increases. SLA increases with maximum temperature of the warmest month, except for regions with warmer temperatures exceeding 35 degrees Celsius, which includes arid environments. However, SLA is inversely proportional to the minimum temperature of the coldest month. For example, tundra vegetation in arctic regions with cold winters shows higher SLA than temperate evergreen forests (Fig. 1).

Plant height increases with annual precipitation and levels off under wetter conditions above 2000  $\text{mm yr}^{-1}$ . Plant height also increases with the maximum temperature of the warmest month, approaching greatest height near 22 °C (tropical regions) and decreasing in areas with very warm temperatures (above 25 °C). Trees also inhabit boreal forests and other areas with cold winters, but canopy height generally increases as the minimum temperature of the coldest month rises (Fig. 1b). Seed mass is most responsive to annual precipitation and the mean temperature of the warmest annual quarter. The log10 of seed mass increases from low to moderate precipitation levels, but declines under higher rainfall amounts (exceeding  $\sim 2700 \text{ mm yr}^{-1}$ ). The mean temperature of the warmest quarter, which generally represents the growing season, has a positive relationship with seed mass except for regions with very warm summer temperatures (exceeding  $\sim 25$  °C) that are associated with lower seed mass plants (Fig. 1c).

The GAM results explain 68.2%, 66.2% and 45.5% of the variance among the SLA, height, and seed mass observations at the global scale (see Table S3 for regression coefficients of the smoothed functions used in the GAM). Using the global extrapolated plant trait information, we show global distribution of plant traits (Fig. 2). High stress areas (deserts and arid regions) are associated with plants with lower height, which is consistent with reported negative effects of low moisture availability on plant height<sup>45</sup>. These areas are also inhabited by plants with lower seed mass, which can promote seed dispersal<sup>16</sup>. Temperate evergreen trees that have high canopy height can enhance their water use efficiency by having low SLA, while also having a longer foliar life span and lower autotrophic respiration cost<sup>46</sup>. Plants in tropical biomes have relatively high values of the three traits, though this region is dominated by plants with greater height and seed mass.

In order to evaluate how vegetation structure and ecosystem productivity may respond as a result of future climate change, we projected the GAM simulated plant traits using climate variables derived from 17 CMIP5 ESMs (Table S2) for the year 2070 based on the RCP8.5 greenhouse gas concentration trajectory<sup>42</sup>. GAM simulations were run on climate variables from each of the 17 ESMs and their ensemble mean. The standard deviation of the

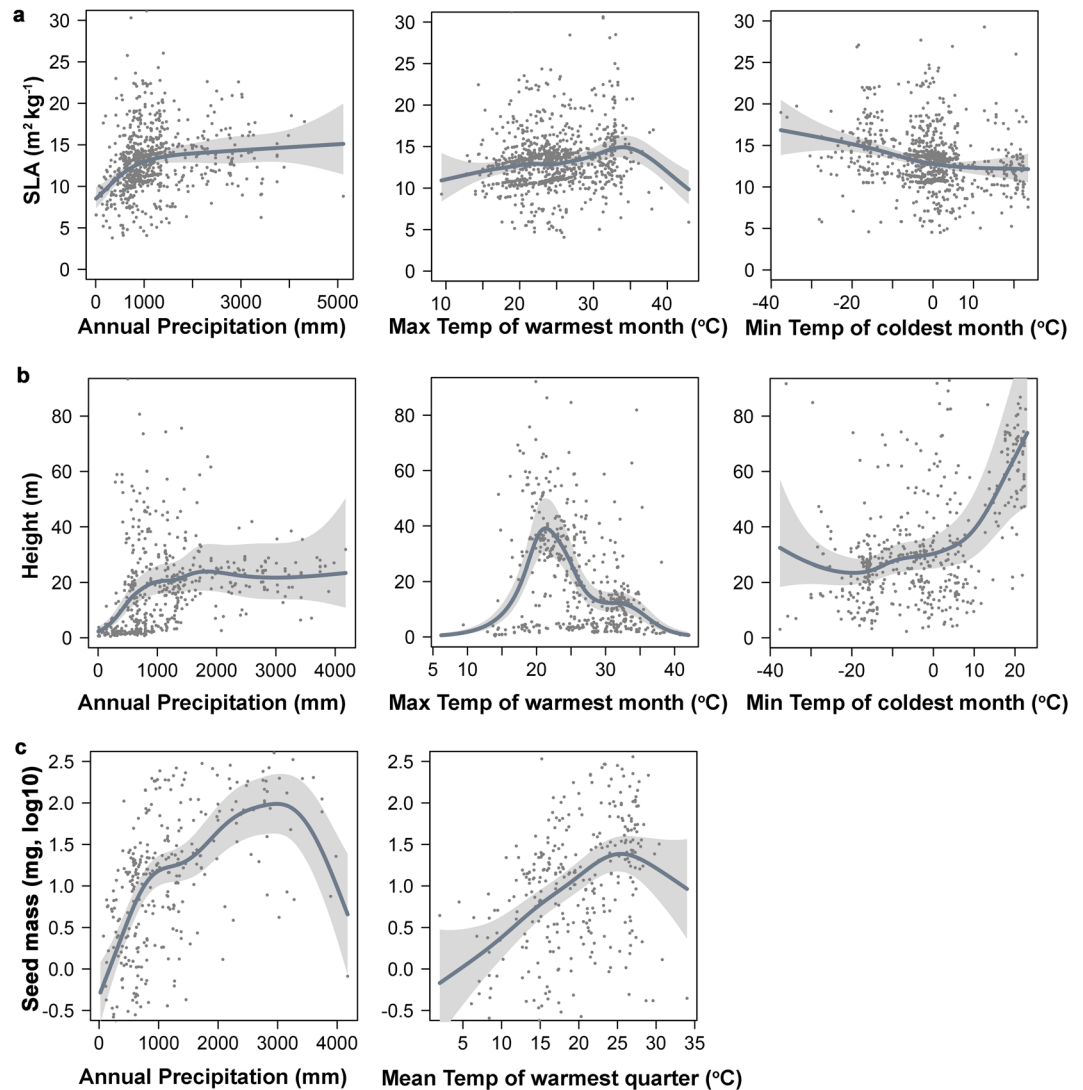


**Figure 1.** The estimated global relationships between the selected key plant trait and best performing climatic predictor variables. Smoothed functions were determined from fitted generalized additive models describing relationships between selected climate drivers and key global plant traits, including SLA (a) canopy height (b) and seed mass (c). The models were developed from climate variables and global plant trait observations including 1178, 329 and 520 data points for SLA, seed mass, and height, respectively. Shaded areas denote 95% confidence intervals, while gray dots represent partial residuals.

resulting GAM outputs derived from 17 ESM climate projection was used as a metric of uncertainty in the model projections. Based on the ensemble projection, boreal and arctic regions show the largest change in plant traits relative to other global biomes, with increases in SLA (+10–20%), canopy height (+20–30%), and seed mass (+25–200%) (Fig. 3). Our results also indicate that in the future, tropical regions may be inhabited by plants with an average  $1 \text{ m}^2 \text{ kg}^{-1}$  (–10%) lower SLA, 5.3 m (–12.5%) lower canopy height, and 0.15 mg (–9.1%) lower log10 seed mass relative to current conditions. These potential changes would not only affect large scale distributions of functional plant traits, but may also affect ecosystem productivity.

We use the GAM framework to explain spatial variation in annual GPP measured from 164 globally distributed flux towers as a function of the selected key plant traits. The resulting model explains 66.4% of the variance in annual GPP among tower sites, resulting in model RMSE performance of  $403 \text{ g C m}^{-2} \text{ yr}^{-1}$  (Figure S7). Model validation using leave-one-out cross validation indicates RMSE performance of  $431 \text{ g C m}^{-2} \text{ yr}^{-1}$ . The GPP model RMSE uncertainty is within approximately 32% of the estimated annual carbon flux. The partial correlation function plots show positive relationships between annual GPP and canopy height and seed mass (Fig. 4). Our results also show that seed mass ( $r^2 = 0.48$ ,  $p < 0.0001$ ) followed by height ( $r^2 = 0.2$ ,  $p < 0.0001$ ), and SLA ( $r^2 = 0.13$ ,  $p = 0.0003$ ) are the best predictors in explaining the variability in ecosystem productivity. Canopy height differentiates between forest and grassland areas, while seed mass distinguishes between plants in more productive (heavier seeds) to less productive regions (lighter seeds)<sup>26,27</sup>. Annual GPP is generally higher in forests than in grassland (high SLA) biomes even though the photosynthetic capacity of forests may be lower<sup>22</sup>. Likewise, while plants with

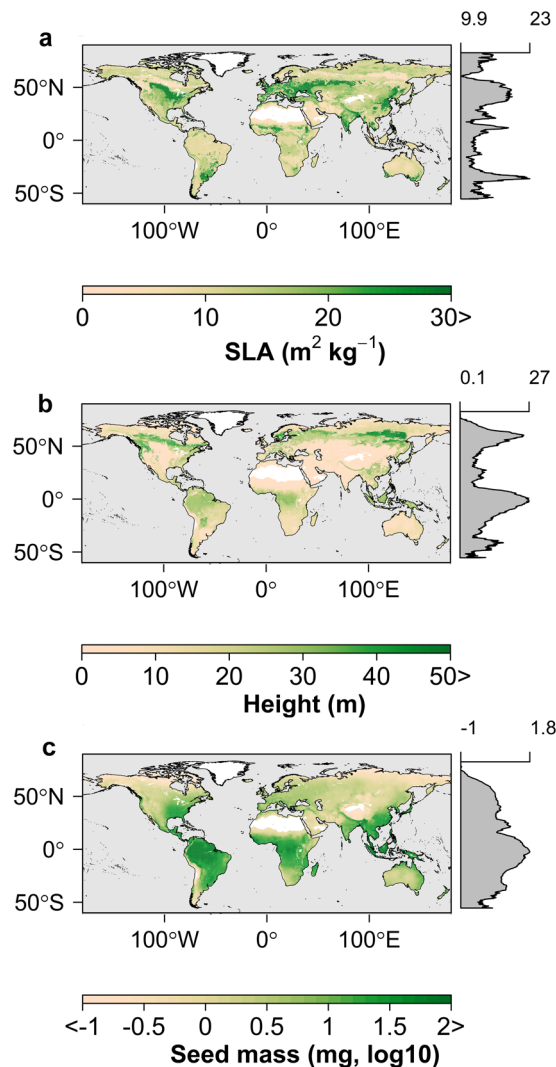


**Figure 2.** Global distribution of the estimated key plant traits. The global distribution of key plant traits (a) Specific Leaf Area (SLA), (b) Height, and (c) Seed Mass (SM)) represent dominant overstorey condition derived from global plant trait observations<sup>40</sup> and gridded climate variables<sup>41</sup>. Gray margins show latitudinal averages for each trait. The figure was created using the rasterVis library<sup>81</sup> in R<sup>77</sup>.

higher SLA tend to have higher leaf nitrogen content and higher photosynthetic capacity<sup>14</sup>, the total productivity of grasslands with high SLA is generally less than forested regions with generally lower SLA (e.g. boreal forests).

We used the predicted plant trait maps under future (2070) climate conditions to estimate the potential ecosystem productivity response to these changes. Our estimation of current global GPP indicates that terrestrial ecosystems can acquire  $134.19 \pm 14.3 \text{ PgC yr}^{-1}$ , while our near future (2070) model projections show a  $7.92 \pm 1.66\%$  decline in global GPP to  $123.56 \pm 13.4 \text{ PgC yr}^{-1}$ . This decline coincides with larger offsetting regional changes in productivity. By 2070, annual GPP above 45 degrees N is expected to increase by 31% ( $+8.1 \pm 0.5 \text{ Pg C}$ ) from current conditions due to greater dominance of trees and shrubs in northern temperate and boreal zones. However, the productivity increase in northern latitudes will be more than offset by a 17.9% GPP decline in the tropics ( $-11.8 \pm 0.84 \text{ PgC yr}^{-1}$ ) as a result of new environmental conditions that will be suitable for trees with shorter height and lower SLA.

With warmer temperatures in arctic and boreal regions, the length of the growing season is expected to increase, relaxing cold temperature constraints in Arctic ecosystems and promoting higher productivity<sup>8,47</sup>. These changes also favor greater leaf area and canopy height, thus promoting a general increase in woody shrubs and trees, consistent with reported northern greening trends indicated from long-term satellite observation records<sup>48</sup> and increased tundra shrub abundance<sup>6</sup>. Our results are also consistent with paleo data records showing that during the Pliocene era, when average global temperatures were as high as what is projected for the near future, the high arctic was a suitable habitat for vascular tree species, including larch, spruce, cedar, alder and birch<sup>49</sup>. Greater tree and shrub dominance in the tundra zone may promote increases in above ground carbon storage over the long-term compared to current conditions. Greater tree and shrub dominance may also alter the land surface albedo in ways that promote further temperature and productivity increases<sup>50</sup>.

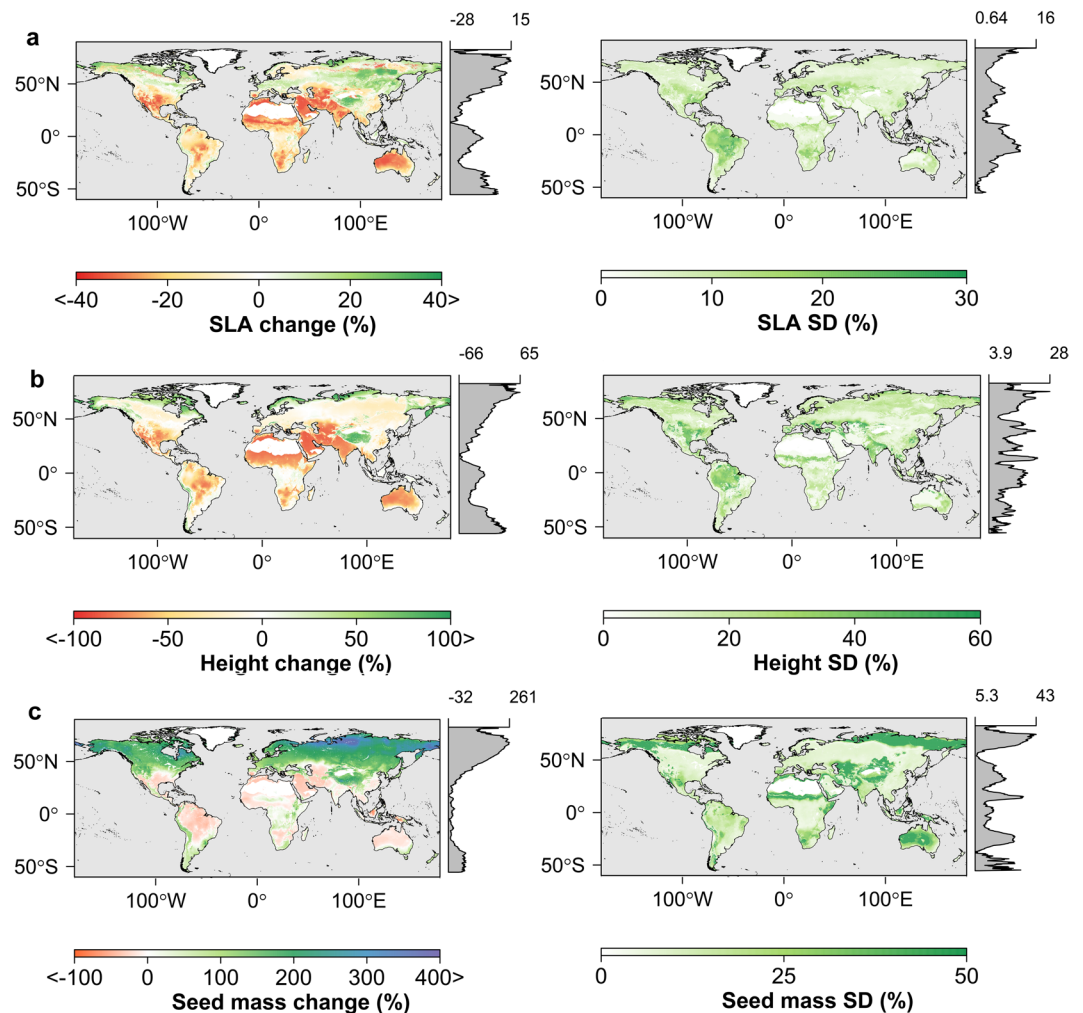


**Figure 3.** Potential changes in key plant traits as a result of projected near-term climate change. GAM projected changes in SLA (a), canopy height (b) and seed mass (c) under future (year 2070) climate conditions represented by the ensemble mean of 17 CMIP5 climate models and RCP 8.5 scenario relative to current conditions; the standard deviation in estimated plant traits derived from each of the 17 climate model outputs is also shown. Gray margins show latitudinal averages (%) for each trait. The figure was created using the rasterVis library<sup>81</sup> in R<sup>77</sup>.

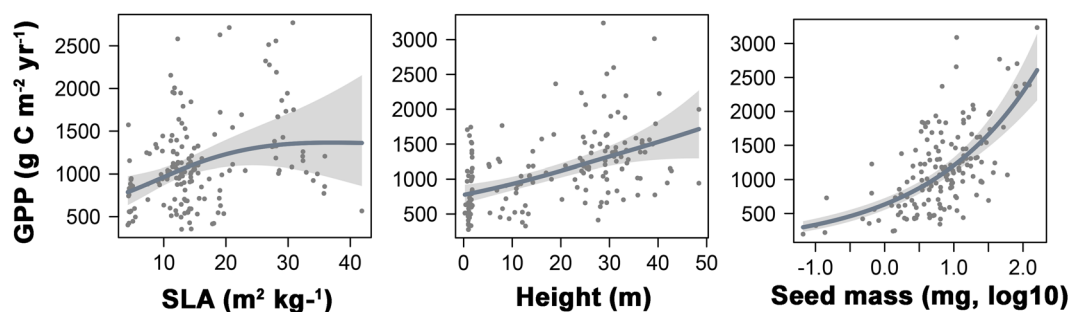


**Figure 4.** Relationships between annual GPP and the estimated key plant traits. The smoothed functions derived from the fitted generalized additive models (GAMs) show the GPP response to variations in the physical plant traits (summary statistics for the smoothed GAM functions are in Table S5). Shaded areas represent the 95% confidence intervals of the functional relationships. Black dots represent partial residuals.

Warmer temperatures and less precipitation in the tropics indicated from the CMIP5 projections are predicted to lead to shorter trees with lower SLA (Fig. 3) consistent with the strong effect of moisture on plant height and on leaf traits related to water conservation. These results are consistent with reported decreases in SLA of tropical

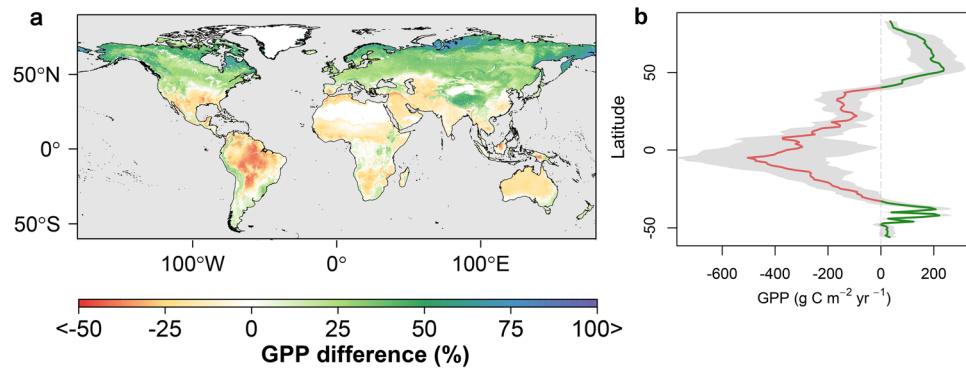


**Figure 5.** Difference in predicted annual GPP between future and current climate conditions. **(a)** The map shows the projected (year 2070) GPP difference from the current productivity estimates, where GPP is estimated using a generalized additive model and plant traits as explanatory variables, and GPP records from 164 global flux tower sites. **(b)** Mean latitudinal distribution (solid line) of the estimated GPP differences between future (2070) and current conditions; gray shading denotes the standard deviation among GPP models estimated using traits predicted from the 17 different climate model projections. Average GPP decreases at low to mid-latitudes, while higher latitude ecosystems show general productivity increases under projected future climate conditions. Figure 5a was created using the rasterVis library<sup>81</sup> in R<sup>77</sup>.

forests as a result of recent environmental change<sup>51</sup>. The projected changes in plant height and SLA favor lower canopy water losses from transpiration, which may have a profound effect on the seasonal water cycle of the Amazon forests as the start of the rainy season is partly due to water transpired by trees<sup>52</sup>. Recent drought events in tropical forests have significantly affected ecosystem productivity<sup>34</sup> and increased the mortality of trees<sup>53</sup>. Our results show the projected changes in GPP and underlying plant traits for the Amazon tropical forests are significantly larger than other tropical forests in Africa and Southeast Asia. The variable response of these tropical ecosystems is consistent with regional differences in hydroclimatic controls on productivity and associated plant community adaptations to drought<sup>54</sup>.

Our results indicate that tropical forests will sequester less carbon in the future than they do now due to shifts in plant community structure driven by a warmer and drier climate (Fig. 5). Our GPP estimates for current climate conditions are in the mid-range of other global GPP estimates derived from multiple models ( $106\text{--}175\text{ Pg C yr}^{-1}$ )<sup>33–36</sup>. However, our GPP estimate is about 20% larger than the average annual productivity level indicated from a satellite remote sensing data record (MODIS-MOD17)<sup>34</sup> and 10% higher than the productivity level indicated from a flux tower up-scaled data record (GPP-MTE)<sup>55</sup> (Figures S7 and S8). We compared our projected future GPP with GPP outputs from five CIMP5 models (Table S8) derived with and without considering CO<sub>2</sub> fertilization effects (Figure S11). In this study, we did not account for the influence of rising atmospheric CO<sub>2</sub> levels on plant productivity, and our trait based GPP focus reflects underlying shifts in plant traits in response to climate. The lack of a direct CO<sub>2</sub> fertilization effect in our predictions may partially account for the lower trait based annual GPP under future climate conditions ( $123.56 \pm 13.4\text{ Pg C}$ ) relative to the average CMIP5 outputs that represent CO<sub>2</sub> fertilization ( $155.24 \pm 27.5\text{ Pg C}$ ). However, our projected future GPP is about 16.7% higher than CIMP5 model GPP estimates that do not consider CO<sub>2</sub> fertilization. The long-term effect of atmospheric CO<sub>2</sub> increases on productivity are not well understood, and ongoing studies, including Free Air CO<sub>2</sub> Enrichment (FACE) experiments, indicate a non-uniform plant response to CO<sub>2</sub> increases<sup>56,57</sup>. However, the plant trait relationship with local climate<sup>15,58–60</sup>, and the alteration of plant species ranges and structural traits as a result of recent climate change has been observed<sup>61</sup>. In arid lands for example, it has been reported that certain shrubs can reduce their size during dry climate conditions<sup>62</sup>. These trait specifications coincide with changes in productivity in arid regions, and contribute to inter-annual variability of the global carbon cycle<sup>63</sup>.

We found that potential shifts in the geography of plant traits strictly as a result of changing climate conditions and habitat suitability contribute to both enhanced ecosystem productivity at higher latitudes, and reduced productivity over lower latitudes. The net effect of these changes with respect to uncertainty in our trait based GPP estimate is a relatively small reduction in global productivity under projected near-term climate change, which represents a departure from a generally increasing productivity trend since the mid-1970s<sup>64</sup>.

Plant productivity has been used as a biospheric indicator of ecosystem goods and services<sup>65</sup>. The estimated shift in GPP patterns indicates potential shifts in ecosystem services for much of the global human population. The recent 2015–2016 extensive drought in Somalia that affected about 3.2 million people due to food insecurity and caused an estimated 766,000 displacements<sup>66</sup> alludes to potential future climate related food insecurity crises at global scales. Based on the current global population distribution<sup>67</sup>, approximately 2.6 billion people are located in areas with projected increases in GPP and could potentially benefit from associated increases in ecosystem goods and services. However, areas with more than five percent projected reduction in GPP are currently inhabited by 4.6 billion people. These areas face potentially higher sustainability risks and security risks exacerbated by both greater ecosystem stress and projected population increases under near future climate.

This study includes several simplifying assumptions that contribute to uncertainty in the model predictions. Potential sources of model uncertainty include our use of a relatively small set of general plant traits to represent

changes in plant community characteristics over a global domain. Our approach is also based on the assumption of stable trait–environment relationships for both spatial and future projections, which may not hold. Under climate change, species may go extinct or adapt to fill new environmental spaces beyond their current niche<sup>37</sup>, which may in turn alter relationships between plant traits and environmental conditions. Our future trait projection model approach also neglects intraspecific variability and species turnover<sup>68</sup> and plant physiological responses and successional processes to changes in climate, which may further affect ecosystem processes including productivity. The use of seed mass (SM) as a driving variable to predict productivity is based on the observed strong empirical correlation between SM and GPP, even though SM is more likely to be a response variable rather than a physical driver of productivity changes. Despite these uncertainties, our results indicate that climate change has the potential to alter plant community structure and the global magnitude and distribution of ecosystem productivity. These changes will influence potential climate feedbacks, plant–animal interactions and ecosystem services. The findings and resulting data products from this research also provide spatially explicit plant trait information that may help to better inform the representation of plant traits in global ecosystem models that extend beyond general assumptions of biome level homogeneity.

## Methods

We used 19 climatic variables from WorldClim database<sup>41</sup> to explain spatial variability in three major physical plant traits informed by the global plant traits database (TRY)<sup>40</sup>. Key plant traits from TRY used in our study included SLA ( $\text{m}^2 \text{kg}^{-1}$ ), tree height (m) and seed mass (mg). The selected WorldClim climatic variables are derived from global average long term (1950–2000) monthly precipitation and mean daily minimum and maximum air temperatures from global weather station records<sup>41</sup>. The climatic variables analyzed included: annual mean temperature and mean diurnal range, Isothermality, temperature seasonality, maximum temperature of the warmest month, minimum temperature of the coldest month, temperature annual range, mean temperature of wettest quarter, mean temperature of driest quarter, mean temperature of warmest quarter, mean temperature of coldest quarter, annual precipitation, precipitation of wettest month, precipitation of driest month, precipitation seasonality, precipitation of wettest quarter, precipitation of driest quarter, precipitation of warmest quarter and precipitation of coldest quarter.

The WorldClim variables are mapped to a global grid at 30 arc-second resolution. These data are spatially interpolated from 47,554 and 24,542 global weather stations for precipitation and temperature, respectively, and have been used extensively for analyzing species habitat relationships and ecological studies (e.g.<sup>69–73</sup>). In this dataset, current climate is characterized by the average of monthly climatic variables from 1950–2000.

We used 204,504 global observations of key plant traits (Figure S1) representing dominant vegetation type characteristics from the TRY database<sup>40</sup>. TRY database covers a high fraction of the most frequent or dominant species available in sPlot<sup>74</sup>, the largest repository for plant community data in the world. To ensure that the trait observations represent global biomes, we used the site level documentation provided in the global plant traits database including woodiness and growth form information to select dominant species traits representing site level plant functional type (PFT) categories that matched collocated general PFT classes represented within a global land cover classification (MODIS MOD12 land cover product<sup>75</sup>). This global selection process resulted in 10,327 SLA observations from 2,343 dominant species, 5,417 plant height observations from 2,188 species, and 2000 seed mass observations from 1,275 species (Table S1, Figure S2) including 6 observations for crops. In the case of multiple observations per location, we used weighted median values of observations based on their functional types, which resulted in 952 observations of seed mass, 1,042 observations of SLA and 1,028 observations of canopy height.

We used a Generalized Additive Model (GAM) framework<sup>43</sup> to describe spatial patterns of plant traits within global biomes, and validated the models using a leave-one-out cross validation method. We assumed that temperature and precipitation are effective proxies for respective energy and water constraints to vegetation processes, and can explain global variability in functional plant traits. We used the visreg library<sup>76</sup> in the R programming environment<sup>77</sup> to show the relationship between response and explanatory variables in our global GAM. This process revealed the relationship between each explanatory and response variable while other covariates were held fixed. The difference between a generalized linear model (GLM) and the GAM approach is that the GAM adds smoothed non-parametric functions to the parametric part of a GLM<sup>43</sup>, allowing for greater flexibility and improved fit<sup>78</sup> in the model structure:

$$g(\mu_i) = X_i^* \theta + f_1(X_{1i}) + f_2(X_{2i}) + f_3(X_{3i}) + \dots \quad (1)$$

where  $\mu_i \equiv E(Y_i)$  and the response variable  $Y_i$  follows an exponential family distribution;  $X_i$  is the  $i^{\text{th}}$  row of the model matrix, and  $\theta$  is a corresponding parameter vector;  $f_j$  are smoothed functions of the covariates in  $X_i$ . Because the PFTs are distinguishable using physical plant traits<sup>23</sup>, we used PFT as a dummy variable in the GAM. In order to minimize co-linearity effects in the regression models, among predictor variables with more than 70% correlation, only one variable was retained, and the rest were excluded from the models. In addition to climatic variables, we used soil attributes including soil organic carbon, clay and silt content, and soil pH to test their predictive power in explaining the variance in trait data, and tested the traits models with and without using the soil attribute data. We optimized the models using stepwise variable selection by means of the AIC to choose the best explanatory variable for prediction of the selected plant traits (Table S4). In order to reduce overfitting of the regression models, we reduced the number of nodes in the smoothed functions and used a restricted maximum likelihood estimator.

Future climate projections are available for climatic variables downscaled from global ESM climate simulations from the recent IPCC CMIP5<sup>79</sup> assessment. We used future ESM climate projections from the RCP 8.5 of the A2 emission scenario<sup>42</sup> (Table S2), where the future climate conditions represent model averages for the

2061–2080 time period centered on year 2070. We used fitted models of the plant traits spanning all vegetated land areas to create global maps of the selected plant traits under current climate (Figure S3), and projected future climate conditions based on each of 17 CMIP5 climate models and their ensemble mean (Figure S5).

We used daily GPP measurements from 164 flux towers from the global FLUXNET network (Table S5) to calculate the annual GPP climatology ( $\text{g C m}^{-2} \text{ yr}^{-1}$ ) for sites representing major global biomes (Figure S4). We explained spatial variability in annual GPP from multi-year observations across the tower sites, using the extrapolated trait maps for current and future climate conditions as explanatory variables (Table S6, Figure S7), and predicted the global annual GPP based on the plant trait distributions (Figure S8) using the GAM. Areas having less than 50 mm of annual precipitation and representing deserts and other barren land were eliminated from the analysis. We also compared the GPP estimates derived from the predicted plant traits information with alternative GAM based GPP predictions derived using only the climate variables (Table S7). Additionally, we compared our GAM predicted annual GPP results with two other global productivity datasets for model verification, including the average annual MODIS MOD17A3 (Collection 5) GPP data record derived at 1-km spatial resolution for the 2000–2014 period<sup>34</sup> and a global tower observation up-scaled GPP record derived at 0.5 degree spatial resolution from 2000–2011 (MTE GPP)<sup>55</sup>. We also calculated the annual GPP spatial means for each 0.05-degree latitudinal bin from these global datasets, while the GPP estimates for future climate conditions were compared against alternative global GPP projections obtained from five CMIP5 global ESMs (Table S8) derived with and without considering  $\text{CO}_2$  fertilization effects.

We acquired global human population data from the NASA Socioeconomic Data and Applications Center (SEDAC)<sup>80</sup>. The SEDAC data provide human population estimates for the year 2000 in each grid cell over the global domain with a 2.5 arc-minute ( $\sim 0.04$  degree) spatial resolution. We classified our global GPP estimates into two regions representing grid cells with at least 5% increase and more than 5% decrease in productivity under projected future (2070) conditions. We then determined the human population densities within each region.

**Data availability.** All data used in this research are publicly available from the cited literature. Results and data products generated from this research are publicly available for download from NTSG and the University of Montana or through contact with the corresponding author.

## References

- Dawson, T. P., Jackson, S. T., House, J. I., Prentice, I. C. & Mace, G. M. Beyond predictions: biodiversity conservation in a changing climate. *Science* **332**, 53–8 (2011).
- Pereira, H. M. *et al.* Scenarios for global biodiversity in the 21st century. *Science* **330**, 1496–501 (2010).
- Moritz, C. & Agudo, R. The future of species under climate change: resilience or decline? *Science* **341**, 504–8 (2013).
- Crimmins, S. M., Dobrowski, S. Z., Greenberg, J. A., Abatzoglou, J. T. & Mynsberge, A. R. Changes in climatic water balance drive downhill shifts in plant species' optimum elevations. *Science* **331**, 324–7 (2011).
- Kelly, A. & Goulden, M. Rapid shifts in plant distribution with recent climate change. *Proc. Natl. Acad. Sci.* **105**, 11823–11826 (2008).
- Myers-Smith, I. H. *et al.* Climate sensitivity of shrub growth across the tundra biome. *Nat. Clim. Chang.* **5** (2015).
- Mcintyre, P. J. *et al.* Twentieth-century shifts in forest structure in California: Denser forests, smaller trees, and increased dominance of oaks. *Proceeding Natl. Acad. Sci.* **112**, 1458–1463 (2014).
- Nemani, R. R. *et al.* Climate-driven increases in global terrestrial net primary production from 1982 to 1999. *Science* **300**, 1560–3 (2003).
- Madani, N., Kimball, J. S., Jones, L. A., Parazoo, N. C. & Guan, K. Global Analysis of Bioclimatic Controls on Ecosystem Productivity Using Satellite Observations of Solar-Induced Chlorophyll Fluorescence. *Remote Sens.* **9**, 1–16 (2017).
- Forkel, M. *et al.* Enhanced seasonal  $\text{CO}_2$  exchange caused by amplified plant productivity in northern ecosystems. *Science* (80-). **4971**, 1–9 (2016).
- Friedlingstein, P. On the contribution of  $\text{CO}_2$  fertilization to the missing biospheric sink. *Global Biogeochem. Cycles* **9**, 541–556 (1995).
- Li, F. Y., Newton, P. C. D. & Lieffering, M. Testing simulations of intra- and inter-annual variation in the plant production response to elevated  $\text{CO}_2$  against measurements from an 11-year FACE experiment on grazed pasture. *Glob. Chang. Biol.* **20**, 228–239 (2014).
- Alan Williams, C. Heat and drought extremes likely to stress ecosystem productivity equally or more in a warmer,  $\text{CO}_2$  rich future. *Environ. Res. Lett.* **9**, 101002 (2014).
- Reich, P. B. Key canopy traits drive forest productivity. *Proc. Biol. Sci.* **1736**, 2128–34 (2012).
- Wright, I. J. *et al.* The worldwide leaf economics spectrum. *Nature* **428**, 821–7 (2004).
- Westoby, M. A leaf-height-seed (LHS) plant ecology strategy scheme. *Plant Soil* **199**, 213–227 (1998).
- Fortunel, C. & Fine, P. V. A. & Baraloto, C. Leaf, stem and root tissue strategies across 758 Neotropical tree species. *Funct. Ecol.* **26**, 1153–1161 (2012).
- Chapin, F. S., Bret-Harte, M. S., Hobbie, S. E. & Zhong, H. Plant functional types as predictors of transient responses of arctic vegetation to global change. *J. Veg. Sci.* **7**, 347–358 (1996).
- Reich, P. B. The world-wide 'fast-slow' plant economics spectrum: a traits manifesto. *J. Ecol.* **102**, 275–301 (2014).
- Wright, I. J. I. & Westoby, M. Leaves at low versus high rainfall: coordination of structure, lifespan and physiology. *New Phytol.* **155**, 403–416 (2002).
- Reichstein, M., Bahn, M., Mahecha, M. D., Kattge, J. & Baldocchi, D. D. Linking plant and ecosystem functional biogeography. *Proc. Natl. Acad. Sci.*, <https://doi.org/10.1073/pnas.1216065111> (2014).
- Madani, N. *et al.* Improving ecosystem productivity modeling through spatially explicit estimation of optimal light use efficiency. *J. Geophys. Res. Biogeosciences* **119**, 1755–1769 (2014).
- Bodegom, P. M. V. *et al.* A fully traits-based approach to modeling global vegetation distribution. *Proc. Natl. Acad. Sci.* **111**, 13733–13738 (2014).
- Verheijen, L. M., Aerts, R., Bönisch, G., Kattge, J. & Van Bodegom, P. M. Variation in trait trade-offs allows differentiation among predefined plant functional types: Implications for predictive ecology. *New Phytologist*, <https://doi.org/10.1111/nph.13623> (2015).
- Reich, P. B. *et al.* Scaling of respiration to nitrogen in leaves, stems and roots of higher land plants. *Ecol. Lett.* **11**, 793–801 (2008).
- Moles, A. T. & Westoby, M. Latitude seed predation and seed mass. *J. Biogeogr.* **30**, 105–128 (2003).
- Santini, B. A. *et al.* The triangular seed mass–leaf area relationship holds for annual plants and is determined by habitat productivity. *Funct. Ecol.* **31**, 1770–1779 (2017).
- Grubb, P. J. & Metcalfe, D. Adaptation and Inertia in the Australian Tropical Lowland Rain-Forest Flora: Contradictory Trends in Intergeneric and Intra-generic Comparisons of Seed Size in Relation to Light Demand. *Funct. Ecol.* **10**, 512–520 (1996).
- Moles, A. T. *et al.* A brief history of seed size. *Science* **307**, 576–80 (2005).



30. Carswell, F. E. *et al.* Photosynthetic capacity in a central Amazonian rain forest. *Tree Physiol.* **20**, 179–186 (2000).
31. Chapin, F. S. I. I., Matson, P. A. & Vitousek, P. M. *Principles of Terrestrial Ecosystem Ecology*. (Springer, 2002).
32. Madani, N., Kimball, J. S. & Running, S. W. Improving Global Gross Primary Productivity Estimates by Computing Optimum Light Use Efficiencies Using Flux Tower Data. *Journal of Geophysical Research: Biogeosciences* **122**, 2939–2951 (2017).
33. Welp, L. R. *et al.* Interannual variability in the oxygen isotopes of atmospheric CO<sub>2</sub> driven by El Niño. *Nature* **477**, 579–82 (2011).
34. Zhao, M. & Running, S. W. Drought-induced reduction in global terrestrial net primary production from 2000 through 2009. *Science* **329**, 940–3 (2010).
35. Anav, A. *et al.* Evaluating the Land and Ocean Components of the Global Carbon Cycle in the CMIP5 Earth System Models. *J. Clim.* **26**, 6801–6843 (2013).
36. Beer, C. *et al.* Terrestrial gross carbon dioxide uptake: global distribution and covariation with climate. *Science* **329**, 834–8 (2010).
37. Dubuis, A. *et al.* Predicting current and future spatial community patterns of plant functional traits. *Ecography (Cop.)*. **36**, 1158–1168 (2013).
38. Verheijen, L. M. *et al.* Inclusion of ecologically based trait variation in plant functional types reduces the projected land carbon sink in an earth system model. *Glob. Chang. Biol.* **21**, 3074–3086 (2015).
39. Verheijen, L. M. *et al.* Impacts of trait variation through observed trait-climate relationships on performance of an Earth system model: A conceptual analysis. *Biogeosciences* **10**, 5497–5515 (2013).
40. Kattge, J. *et al.* TRY - a global database of plant traits. *Glob. Chang. Biol.* **17**, 2905–2935 (2011).
41. Hijmans, R. J. *et al.* Very high resolution interpolated climate surfaces for global land areas. *Int. J. Climatol.* **25**, 1965–1978 (2005).
42. Riahi, K., Grübler, A. & Nakicenovic, N. Scenarios of long-term socio-economic and environmental development under climate stabilization. *Technol. Forecast. Soc. Change* **74**, 887–935 (2007).
43. Wood, S. N. *Generalized Additive Models: An Introduction with R. Texts in Statistical Science* (Chapman & Hall/CRC, 2006).
44. Burnham, K. P. & Anderson, D. R. *Model Selection and Multimodel Inference: A Practical Information-Theoretic Approach*. **172**, (Springer New York, 2002).
45. Klein, T., Randin, C. & Körner, C. Water availability predicts forest canopy height at the global scale. *Ecol. Lett.* **18**, 1311–1320 (2015).
46. Reich, P. B., Rich, R. L., Lu, X., Wang, Y.-P. & Oleksyn, J. Biogeographic variation in evergreen conifer needle longevity and impacts on boreal forest carbon cycle projections. *Proc. Natl. Acad. Sci.* **111**, 17684–17684 (2014).
47. Kim, Y., Kimball, J. S., Zhang, K. & McDonald, K. C. Satellite detection of increasing Northern Hemisphere non-frozen seasons from 1979 to 2008: Implications for regional vegetation growth. *Remote Sens. Environ.* **121**, 472–487 (2012).
48. Zhu, Z. *et al.* Greening of the Earth and its drivers. 1–6, <https://doi.org/10.1038/nclimate3004> (2016).
49. Csank, A. Z. *et al.* Estimates of Arctic land surface temperatures during the early Pliocene from two novel proxies. *Earth Planet. Sci. Lett.* **304**, 291–299 (2011).
50. Chapin, F. S. *et al.* Role of land-surface changes in arctic summer warming. *Science* **310**, 657–60 (2005).
51. van der Sande, M. T. *et al.* Old growth Neotropical forests are shifting in species and trait composition. *Ecol. Monogr.* **86**, 228–243 (2016).
52. Fu, R. & Li, W. The influence of the land surface on the transition from dry to wet season in Amazonia. *Theor. Appl. Climatol.* **78**, 97–110 (2004).
53. Phillips, O. L. *et al.* Drought-mortality relationships for tropical forests. *New Phytol.* **187**, 631–46 (2010).
54. Guan, K. *et al.* Photosynthetic seasonality of global tropical forests constrained by hydroclimate. *Nat. Geosci.* 284–289, <https://doi.org/10.1038/NGEO2382> (2015).
55. Jung, M. *et al.* Global patterns of land-atmosphere fluxes of carbon dioxide, latent heat, and sensible heat derived from eddy covariance, satellite, and meteorological observations. *J. Geophys. Res.* **116**, 1–16 (2011).
56. Körner, C. *et al.* Carbon flux and growth in mature deciduous forest trees exposed to elevated CO<sub>2</sub>. *Science (80-)*. **309**, 1360–1362 (2005).
57. Ainsworth, E. A. & Long, S. P. What have we learned from 15 years of free-air CO<sub>2</sub> enrichment (FACE)? A meta-analytic review of the responses of photosynthesis, canopy properties and plant production to rising CO<sub>2</sub>. *New Phytol.* **165**, 351–372 (2005).
58. Díaz, S. *et al.* The global spectrum of plant form and function. *Nature* **529**, 1–17 (2015).
59. Ordoñez, J. C. *et al.* A global study of relationships between leaf traits, climate and soil measures of nutrient fertility. *Glob. Ecol. Biogeogr.* **18**, 137–149 (2009).
60. Wright, I. J. *et al.* Global climatic drivers of leaf size. *Science (80-)*. **12**, 917–921 (2017).
61. Chen, I., Hill, J. K., Ohlemüller, R., Roy, D. B. & Thomas, C. D. Rapid range shifts of species of climate warming. *Science (80-)*. **333**, 1024–1026 (2011).
62. Salguero-Gomez, R., Siewert, W., Casper, B. B. & Tielborger, K. A demographic approach to study effects of climate change in desert plants. *Philos. Trans. R. Soc. B Biol. Sci.* **367**, 3100–3114 (2012).
63. Poulter, B. *et al.* Contribution of semi-arid ecosystems to interannual variability of the global carbon cycle. *Nature* **509**, 600–3 (2014).
64. Ballantyne, aP., Alden, C. B., Miller, J. B., Tans, P. P. & White, J. W. C. Increase in observed net carbon dioxide uptake by land and oceans during the past 50 years. *Nature* **488**, 70–72 (2012).
65. Running, S. W. A Measurable Planetary Boundary for the Biosphere. *Science (80-)*. **337**, 1458–1459 (2012).
66. OCHA. Somalia: Humanitarian Snapshot (2017). Available at: <http://www.unocha.org>. (Accessed: 8th March 2017).
67. CIESIN (Center for International Earth Science Information Network). Gridded population of the world: future estimates. Socioeconomic Data and Applications Center (SEDAC) Columbia University Palisades New York. Accessed August 2016 (2005).
68. Gibson-Reinemer, D. K., Sheldon, K. S. & Rahel, F. J. Climate change creates rapid species turnover in montane communities. *Ecol. Evol.* **5**, 2340–2347 (2015).
69. Pearson, R. G. *et al.* Shifts in Arctic vegetation and associated feedbacks under climate change. *Nat. Clim. Chang.* **3**, 673–677 (2013).
70. Anadon, J. D. J., Sala, O. E. O. & Maestre, F. T. F. Climate change will increase savannas at the expense of forests and treeless vegetation in tropical and subtropical Americas. *J. Ecol.* **102**, 1363–1373 (2014).
71. Morin, X. & Lechowicz, M. J. Niche breadth and range area in North American trees. *Ecography (Cop.)*. **36**, 300–312 (2013).
72. Saatchi, S. *et al.* Mapping landscape scale variations of forest structure, biomass, and productivity in Amazonia. *Biogeosciences Discuss.* **6**, 5461–5505 (2009).
73. Fritz, S. *et al.* Mapping global cropland and field size. *Glob. Chang. Biol.* **21**, 1980–1992 (2015).
74. Dengler, J. *et al.* sPlot - the new global vegetation-plot database for addressing trait-environment relationships across the world's biomes. *Biodivers. Veg. pattern, Process. Conserv.* **90**, <https://doi.org/10.13140/RG.2.1.1979.0164> (2014).
75. Friedl, M. A. *et al.* MODIS Collection 5 global land cover: Algorithm refinements and characterization of new datasets. *Remote Sens. Environ.* **114**, 168–182 (2010).
76. Breheny, P. & Burchett, W. visreg: Visualization of Regression Models. R package version 2.2–0 (2015).
77. R Core Team. R: A language and environment for statistical computing (2016).
78. Guisan, A., Edwards, T. C. & Hastie, T. Generalized linear and generalized additive models in studies of species distributions: setting the scene. *Ecol. Modell.* **157**, 89–100 (2002).
79. Stocker, T. F. *et al.* *Climate Change 2013 The Physical Science Basis: Working Group I Contribution to the Fifth Assessment Report of the Intergovernmental Panel on Climate Change* (2013).

80. Center for International Earth Science Information Network - CIESIN - Columbia University, United Nations Food and Agriculture Programme - FAO, and Centro Internacional de Agricultura Tropical - CIAT Gridded Population of the World, Version 3 (GPWv3): Population Count Grid (2005).
81. Hijmans, R. & Lamigueiro, O. P. *MeteoForecast*. R package version 0.43 (2016).

## Acknowledgements

This study was conducted with funding provided by NASA (NNX15AB59G, NNX14AI50G). Additional support was provided by the TRY initiative on plant traits (<http://www.try-db.org>). This work used eddy covariance data acquired by the FLUXNET community. For their roles in producing, coordinating, and making available the CMIP5 model output, we acknowledge the climate modeling groups (listed in table S1 of this paper), the World Climate Research Programme's (WCRP) Working Group on Coupled Modelling (WGCM), and the Global Organization for Earth System Science Portals (GO-ESSP).

## Author Contributions

N.M. implemented the analysis and led in the design and writing of the paper. J.S.K., A.P.B., D.L.R.A., P.M.B., P.B.R., J.K., A.S., M.N., M.O.J., M.Z., S.W.R. contributed to writing and provided feedback on development of the research.

## Additional Information

**Supplementary information** accompanies this paper at <https://doi.org/10.1038/s41598-018-21172-9>.

**Competing Interests:** The authors declare no competing interests.

**Publisher's note:** Springer Nature remains neutral with regard to jurisdictional claims in published maps and institutional affiliations.



**Open Access** This article is licensed under a Creative Commons Attribution 4.0 International License, which permits use, sharing, adaptation, distribution and reproduction in any medium or format, as long as you give appropriate credit to the original author(s) and the source, provide a link to the Creative Commons license, and indicate if changes were made. The images or other third party material in this article are included in the article's Creative Commons license, unless indicated otherwise in a credit line to the material. If material is not included in the article's Creative Commons license and your intended use is not permitted by statutory regulation or exceeds the permitted use, you will need to obtain permission directly from the copyright holder. To view a copy of this license, visit <http://creativecommons.org/licenses/by/4.0/>.

© The Author(s) 2018